ring polymer

Theoretical study on the mechanism of double proton transfer in porphycene by path-integral molecular dynamics simulations

Takehiro Yoshikawa [a], Shuichi Sugawara [a], Toshiyuki Takayanagi [a,*], Motoyuki Shiga [b], Masanori Tachikawa [c]

[a] Department of Chemistry, Saitama University, Saitama City, Saitama 338-8570, Japan
[b] Center for Computational Science and E-systems, Japan Atomic Energy Agency, Higashi-Ueno 6-9-3, Taito-ku, Tokyo 110-0015, Japan
[c] Quantum Chemistry Division, Graduate School of Nanobioscience, Yokohama-City University, Seto 22-2, Kanazawa-ku, Yokohama 236-0027, Japan

ABSTRACT

Full-dimensional path-integral molecular dynamics simulations were performed to determine whether the double proton transfer tautomerization of porphycene is a concerted or a stepwise process. We employed an on-the-fly direct dynamics technique at the semiempirical PM6 method whose parameters were determined so as that the relative energies of the stationary points approximately reproduce previously reported electronic structure calculations. It was found that double proton transfer occurs dominantly through the concerted pathway via the second-order saddle point structure and that contribution of the stepwise mechanism increases with a temperature increase. Nuclear quantum effects play essential roles in determining the proton transfer mechanism.

© 2010 Elsevier B.V. All rights reserved.

1. Introduction

It is quite well-known that multiple proton/hydrogen transfer, which is one of the most investigated chemical reactions, plays a very important role in many physical, chemical and biological processes [1,2]. For cases involving more than one proton, a fundamental question to be solved is whether the transfer occurs in a concerted or stepwise manner. Porphycene, which is a constitutional isomer of porphyrin, is a suitable molecule for studying the detailed mechanism of double proton transfer processes. This molecule has four pyrrole ring that form four protonable sites inside an inner cavity. Since only two of these can be protonated at any instant of time, there exist several possible tautomeric forms. The tautomerization of porphycene is summarized in Fig. 1, which is showing the proton transfer pathways among the lowest four stationary points on the ground-state potential energy surface. All previous electronic structure calculations show that the C_{2h} *trans* structure is the most stable tautomer and that the energy of the C_{2v} *cis* structure is slightly higher than that of the *trans* structure [3–14]. Thus, the C_{2v} *cis* configuration is the intermediate on the potential energy surface. The D_{2h} SS structure is a second-order saddle point (or hilltop) and is the most probable transition state along the concerted double proton transfer pathway between the two *trans* structures. The C_s TS structure is the transition state (first-order saddle point) of the stepwise single proton transfer process between the *trans* and *cis* configurations. It should be mentioned that all the electronic structure levels give the barrier for the concerted pathway to be higher than that along the stepwise pathway. For example, Kozlowski and Zgierski have reported the barrier heights of D_{2h} SS and C_s TS structures to be 7.6 and 4.9 kcal/mol, respectively, at the B3LYP/TZ2P level of theory [6]. However, it should be emphasized that inclusion of harmonic vibrational zero-point energy significantly changes the energetics of the two reaction pathways, as already noted by Kozlowski and Zgierski [6]. They have shown that the barrier heights of the two reaction pathways are comparable (1.6 kcal/mol) after zero-point energy correction at the same B3LYP/TZ2P level. This is simply due to the fact that the D_{2h} SS structure has one more imaginary frequency than C_s TS. Consequently, in order to understand the detailed mechanism of the double proton transfer process in porphycene, one has to employ molecular dynamics theories including nuclear degrees of freedom. In particular, it is expected that nuclear quantum effects of hydrogen atoms may play essential role in such light atom transfer processes.

It should be mentioned that various experimental studies [15–20] have already been reported for proton transfer in porphycene after the first synthesis of porphycene by Vogel et al. [21]. For example, the motion of the inner two protons is too rapid to be frozen in the NMR time scale even at temperature of 106 K [15]. Electronic absorption and fluorescence spectra have been measured by Sepioł et al. for porphycene isolated in low-temperature supersonic molecular beams [17]. Their study clearly revealed quantum delocalization of the inner two protons by observing the tunneling doublet structure with a splitting of 4.4 cm^{-1}. Very recently, a high-resolution spectroscopic technique using low-temperature helium nanodroplets has been applied for porphycene and its deuterated compounds [20]. It was found that tunneling
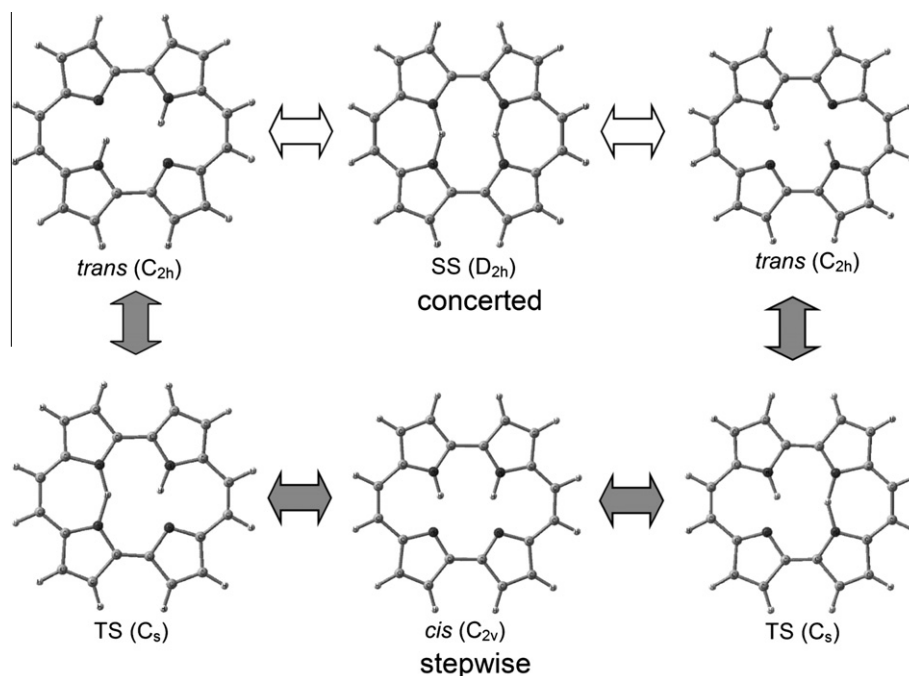
Fig. 1. Concerted (C_{2h} trans ↔ D_{2h} SS ↔ C_{2h} trans) and stepwise (C_{2h} trans ↔ C_s TS ↔ C_{2v} cis) double proton transfer pathways for the tautomerism in porphycene.

splitting values were strongly dependent on vibrational excitation; a mode-selective promotion or inhibition of the tunneling probability was observed. This result demonstrates a multidimensional character of the double proton transfer processes in porphycene.

In this Letter we report results of full-dimensional path-integral molecular dynamics (PIMD) simulations for porphycene. In the PIMD method, the quantum mechanical character of nuclei is described by a cyclic chain polymer composed of classical quasi-particles which are frequently called beads. With the PIMD formalism, one can easily obtain thermal equilibrium structures of molecules including both quantum mechanical motions and thermal fluctuations of nuclei. The most robust approach would be 'on-the-fly' ab initio PIMD [22–25], where ab initio electronic structure theory calculations are directly employed to obtain potential energy values and their derivatives during the course of the PIMD propagation. However, it is still very expensive to use ab initio PIMD methods for the present porphycene system. In this work, in order to reduce computational time, we have alternatively decided to employ the semiempirical electronic structure method with specific reaction parameters (SRP) [26–28] which are obtained by adjusting the semiempirical parameters to reproduce the energetics by quantum chemistry electronic structure calculations. It should be noted that a typical CPU time for obtaining the potential energy and its gradients at a given molecular geometry with the semiempirical method is much faster than that with the standard DFT method by a factor of 10^2–10^3. This allows us to obtain statistically enough sampling for discussing detailed proton transfer mechanisms within reasonable computational costs. The goal of this work is to understand whether double proton transfer occurs through concerted or stepwise pathways and to understand the temperature dependence of the proton transfer mechanism from a theoretical point of view.

2. Computational method

The semiempirical PM6 Hamiltonian [29] was used as a starting point for the SRP adjustments. Since it has been previously pointed out that porphycene (and other porphyrinoids) is an example for a
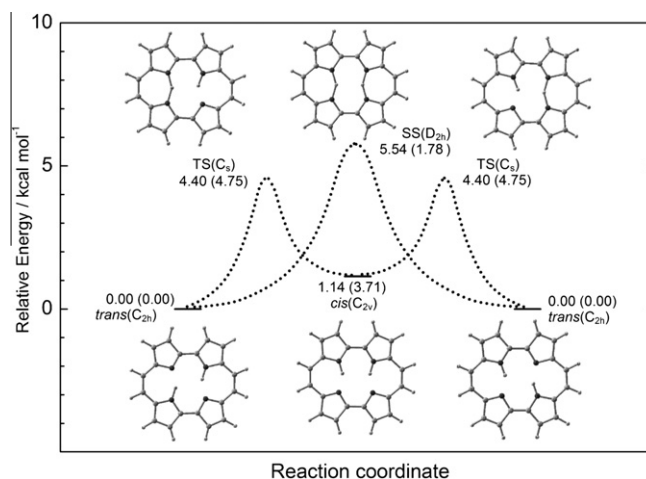

Fig. 2. Schematic energy diagram of the double proton transfer processes in porphycene at the PM6-SRP level.

Table 1
Original PM6 parameters and specific reaction parameters determined in this work for porphycene.

Atom	Parameter	PM6	PM6-SRP	Δ
H	U_{SS} (eV)	−11.2470	−10.8118	0.4352
	β_S (eV)	−8.3530	−8.0180	0.3350
	G_{SS} (eV)	14.4487	14.7724	0.3237
	a_1 (none)	0.0242	0.0357	0.0115
	b_1 (Å^{-2})	3.0560	5.2628	2.2068
	c_1 (Å)	1.7860	1.9837	0.1977
C	U_{SS} (eV)	−51.0897	−51.0995	−0.0098
	U_{PP} (eV)	−39.9379	−39.9334	0.0045
	β_S (eV)	−15.3852	−15.7835	−0.3983
	β_P (eV)	−7.4719	−7.5395	−0.0676
	G_{SS} (eV)	13.3355	13.5478	0.2123
	G_{PP} (eV)	10.7783	10.0116	−0.7667
	G_{SP} (eV)	11.5281	11.9605	0.4324
	G_{P2} (eV)	9.4862	9.6319	0.1457
	H_{SP} (eV)	0.7173	0.3891	−0.3282

Table 2
Comparison of relative energies (in kcal/mol) between stationary points on the porphycene potential energy surface obtained with various electronic structure levels of theory. Numbers in parentheses are relative energies including zero-point vibrational energy correction obtained from harmonic vibrational frequency analyses. The relative energy of *trans*-porphycene (C_{2h}) is taken to be zero.

Level	*trans* (C_{2h})	*cis* (C_{2v})	TS (C_s)	SS (D_{2h})
B3LYP/6-31G(d)[a]	0.0 (0.0)	2.6 (2.1)	5.4 (2.1)	8.2 (2.2)
B3LYP/6-31G(d, p)[b,e]	0.0 (0.0)	2.23 (1.59)	4.10 (1.01)	6.13 (0.55)
B3LYP/6-31+G(d, p)[c]	0.0 (0.0)	2.30 (0.59)	4.68 (5.54)	6.45 (3.03)
B3LYP/TZ2P[a]	0.0 (0.0)	2.4 (1.9)	4.9 (1.6)	7.6 (1.6)
PZB/PW[d]	0.0	2.5	4.9	7.5
BLYP/PW[d]	0.0	2.1	3.9	5.9
PBE/PW[d]	0.0	1.5	2.4	3.5
BP/PW[d]	0.0	1.6	2.5	3.6
MP2/6-31G(d)[a]	0.0 (0.0)	5.1 (4.6)	5.7 (2.4)	7.6 (1.6)
MP2/6-31+G(d, p)[c]	0.0	2.65	3.75	5.23
MPW1K/6-31+G(d, p)[c]	0.0	1.68	2.42	3.41
SCC-DFTB[b]	0.0	3.7	11.1	
PM3[e]	0.0 (0.0)	6.07 (6.09)	18.51 (14.43)	29.81 (22.08)
PM6[e]	0.0 (0.0)	5.71 (5.79)	10.87 (8.03)	12.38 (7.47)
PM6-SRP[e]	0.0 (0.0)	1.14 (3.71)	4.40 (4.75)	5.54 (1.78)

[a] Ref. [6].
[b] Ref. [10].
[c] Ref. [11].
[d] Ref. [12].
[e] This work.

system with a Hartree–Fock instability [30], we have employed the unrestricted Hartree–Fock (UHF) method throughout the present semiempirical molecular orbital calculations. The scheme of the SRP adjustments employed in this study is somewhat different from the usual scheme, where semiempirical parameters are optimized by minimizing the target functional value representing a measure of the difference between ab initio electronic structure properties (energy, geometric parameters or vibrational frequencies) and the corresponding values obtained with semiempirical method. In an early stage of the present investigation, we have found that the unrestricted PM6 method using the original parameters gives relatively reasonable geometries and vibrational properties for the four stationary points (see Fig. 2) on the ground-state potential energy surface. The only difference was the relative energies for these stationary points (see Table 2). In order to obtain reasonable energetics values, we have randomly generated trial semiempirical parameters within appropriate ranges and then performed geometry optimization of the four stationary points. More specifically, in the case of the parameters used in molecular integrals, we generated a trial value in the range of $(-1 + \alpha)$ and $(\alpha + 1)$ eV, where α is the original PM6 parameter. In the case of the three parameters for the gaussian function used in the core–core repulsion energy [29], we have generated trial values within ±150%. A total of 200 sets of parameters were randomly generated and then the energetics obtained were compared to that obtained from various electronic structure calculations. The parameters we have finally chosen are summarized in Table 1 along with the PM6 original parameters. Table 2 compares the PM6-SRP relative energies of the four stationary points to those obtained by various electronic structure levels. It is seen that the PM6-SRP method gives reasonable agreement with previous DFT results at the B3LYP, BLYP, PBE, BP and MPW1K levels of theory. Fig. 3 compares some PM6-SRP geometric parameters to those obtained at the B3LYP/TZ2P [6] and MP2/6-31+G(d, p) levels. Geometric parameters at the MP2/6-31+G(d, p) level were obtained in this study using the Gaussian03 package program [31] since only the energetic at the same level been were reported in Ref. [10].

On-the-fly imaginary-time PIMD simulations [22–25,32] have been performed to calculate thermal equilibrium structures of the porphycene molecule on the PM6-SRP potential energy surface. Potential energy and gradient values were directly calculated using the MOPAC2007 code [33] at each time step. The massive Nose–Hoover chain technique in the velocity Verlet algorithm with time increment being Δt = 5–10 au (0.12–0.24 fs) was used to control the system temperature. The PIMD simulations were performed with 40 and 24 cyclic beads at T = 300 K and 500 K, respectively. The total steps were taken to be 500 000 steps for both temperatures. These numerical parameters were carefully chosen after preliminary convergence tests. The details of our computational method are described in Refs. [23–25].

3. Results

Fig. 4 displays a representative three-dimensional perspective plot of the nuclear distribution function for the porphycene molecule obtained from the PIMD simulation at T = 300 K. In this plot, Cartesian coordinates are transformed so as that overall translational and rotational motions are removed. Large fluctuation motion can be seen for all hydrogen atoms due to the large zero-point vibrational amplitude of light atoms. However, qualitative trend in their motions is clearly different between the outer and inner hydrogen atoms. We can see that out-of-plane motions are significant for the outer 12 hydrogen atoms, while the inner two hydrogen atoms are mainly vibrating within the molecular plane due to hydrogen-bonding although small out-of-plane amplitudes are also seen. Another interesting point seen in Fig. 4 is that fluctuations of the inner nitrogen atoms are quite small compared to those of the outer carbon atoms despite the fact that the corresponding masses are nearly the same. Out-of-plane fluctuations can be clearly seen for the carbon atoms similar to those of the outer hydrogen atoms. On the other hand, the vibrational amplitudes for the nitrogen atoms are seen to be small. This may be presumably because the motions of the inner nitrogen atoms are spatially restricted due the strong hydrogen-bonding of the inner hydrogen atoms. For this reason, one can notice that the molecular frame made by the four nitrogen atoms as well as by the inner cavity hydrogen atoms is quite rigid.

Fig. 5 shows the two-dimensional contour plots of the inner proton distributions as a function of the $r_1 - r_2$ and $r_3 - r_4$ coordinates obtained from the PIMD simulations at T = 300 and 500 K. Notice that the coordinate origin ($r_1 - r_2 = r_3 - r_4 = 0$) corresponds
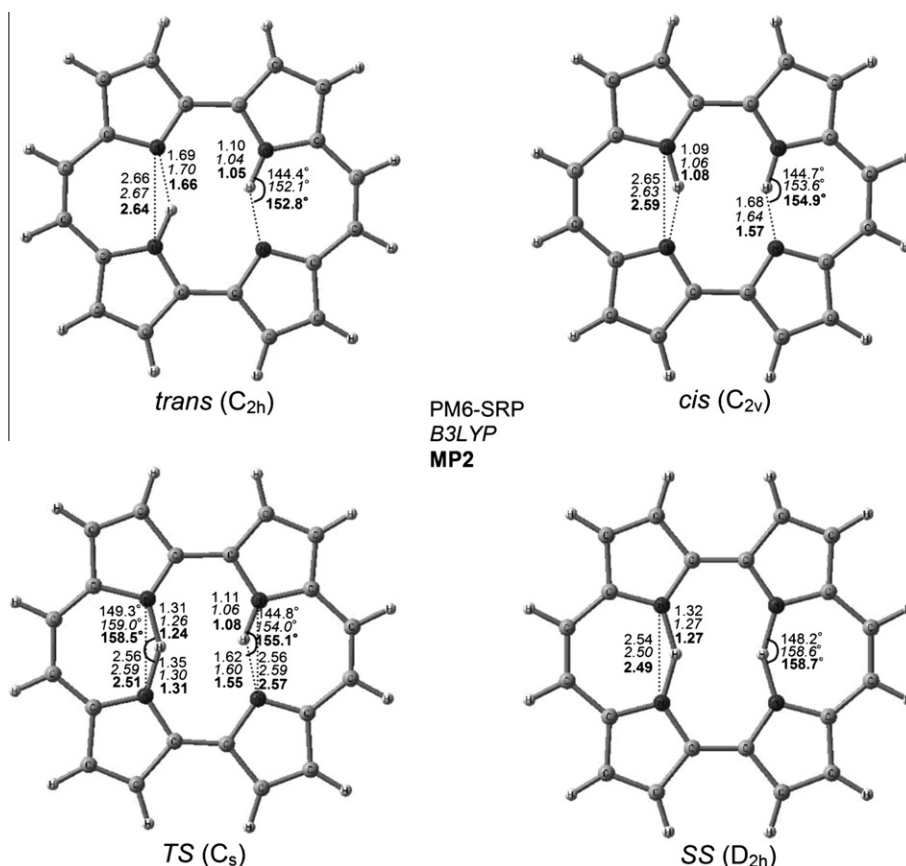
Fig. 3. Comparison of the optimized PM6-SRP stationary point geometries on the potential energy surface for porphycene to the B3LYP/TZ2P [6] (italic) and MP2/6-31+G(d, p) (bold) results. Selected bond lengths (in Å) and bond angles (in degrees) are shown.
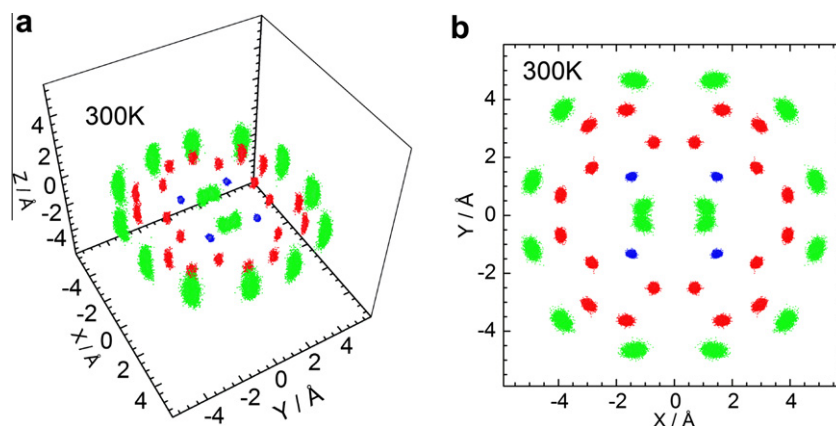

Fig. 4. (a) Three-dimensional perspective plot of the nuclear distribution of porphycene calculated from the PIMD simulations at $T = 300$ K on the PM6-SRP potential energy surface. (b) Projected plot on the x–y plane.

to the D_{2h} second-order saddle point structure of porphycene (see Figs. 1 and 3). From the density distribution plots presented in Fig. 5a, it is seen that double proton transfer between *trans–trans* structures in porphycene at $T = 300$ K occurs mainly through the concerted mechanism due to the higher distribution around the coordinate origin, $(r_1 - r_2, r_3 - r_4) = (0, 0)$. At $T = 300$ K the population of the *cis* form is seen to be very small. Thus, the contribution of the stepwise mechanism is less important. On the other hand, one can notice that the population of the *cis* form clearly increases at $T = 500$ K. Therefore, we can see that the double proton transfer reaction also occurs via the stepwise mechanism from the density

plot present in Fig. 5b although the dominant mechanism is the concerted one.

It should be emphasized that the trend seen in Fig. 5 can qualitatively be predicted from the zero-point corrected barrier heights; however, the present PIMD result definitely indicates the importance of the vibrational quantization for understanding the double proton transfer mechanism in porphycene. In order to understand the importance of the nuclear quantum effect, we have also performed standard constant temperature classical molecular dynamics simulations on the same PM6-SRP potential energy surface. The classical result is presented in Fig. 5c. Notice that
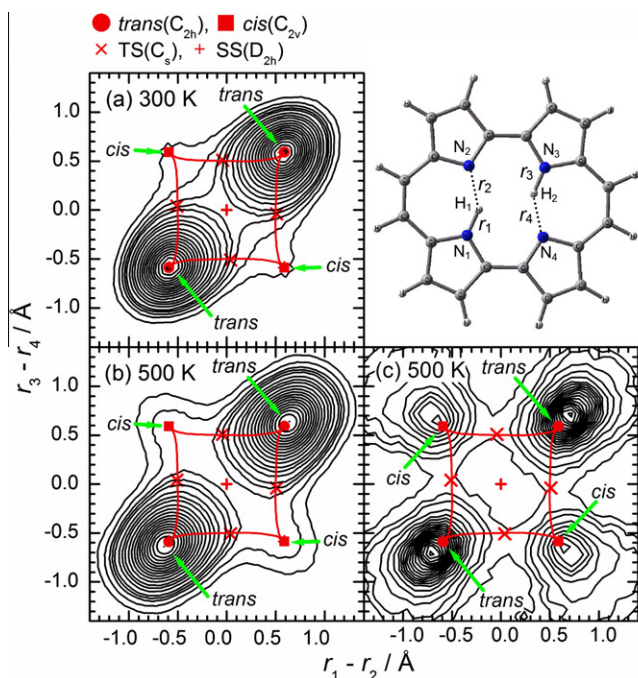
Fig. 5. Two-dimensional contour plots of the inner proton distributions in porphycene as a function of $r_1 - r_2$ and $r_3 - r_4$ obtained from the PIMD simulations at $T = 300$ K (a) and $T = 500$ K (b). The same plot but obtained from the classical MD simulation at $T = 500$ K is shown in (c). Circles and squares indicate C_{2h} trans or C_{2v} cis minima on the PM6-SRP potential energy surface, respectively. The saddle points for the stepwise process and the second-order saddle point for the concerted process are also shown as crosses. The intrinsic reaction coordinates (IRCs) for the stepwise pathways are also shown.

the classical distribution function is completely different from the quantum distributions. In the classical case, we have found that the double proton transfer process always occurs via the C_s first-order saddle point structure, i.e., via the stepwise mechanism. Therefore, we conclude that the dominant concerted double proton transfer mechanism is a result of nuclear quantum effects.

Fig. 6 displays the two-dimensional contour plots of the inner proton distribution as a function of the N_1-N_2 (or N_3-N_4) distance
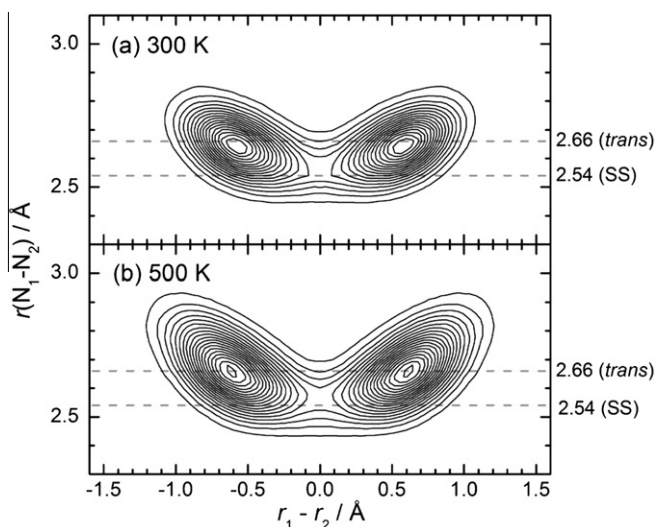

Fig. 6. Two-dimensional contour plots of the proton distribution in porphycene as a function of the N_1-N_2 distance and the difference between H_1-N_1 and H_1-N_2 distances obtained from the PIMD simulations at (a) $T = 300$ K and (b) $T = 500$ K. Horizontal lines indicate the N–N distances at the trans equilibrium structure and the SS saddle point.

and $r_1 - r_2$ (or $r_3 - r_4$). Since the $r_1 - r_2$ distance difference qualitatively corresponds to the reaction coordinate of proton transfer, these plots indicate that the proton transfer process strongly correlates with the N_1-N_2 stretch motion. We can see that proton transfer effectively occurs when the N_1-N_2 distance is small indicating that the N–N stretch vibration is a promoting mode of proton transfer, as expected. This behavior is frequently seen in the proton transfer process in water [34]. However, note that the N–N distance difference between the transition state and the equilibrium structures (0.12 Å) is not so large as the case of O–O distance of water.

4. Discussion

In this work we have performed full-dimensional PIMD simulations for porphycene in order to understand the detailed mechanism of the inner double proton tautomerism from a quantum mechanical viewpoint. We have employed the PM6-SRP semiempirical potential energy surface where the semiempirical parameters have been chosen so as that the obtained potential surface gives reasonable agreement with the previous DFT energetics. The present quantum simulations clearly show that the double proton transfer process in porphycene takes place dominantly via the concerted mechanism especially at low-temperatures. More importantly, nuclear quantum effects play essential roles in determining the mechanism of the double proton transfer dynamics at least for a given potential energy surface. We have also found that the contribution of the stepwise mechanism via the cis configuration increases as the temperature increases.

Although the present PIMD simulations provide interesting information on the quantum nature of the double proton transfer processes in porphycene, it should be emphasized that the PIMD results do not contain time-dependent dynamical information since the PIMD simulations give only quantum statistical distributions for nuclei. In fact, the 'concerted mechanism' can be further divided into concerted synchronous and asynchronous processes depending on the time delay of the two proton motions [14]. Although it may be inappropriate to give a time-dependent picture of the two inner proton dynamics from the present PIMD results, it is interesting to notice that the nuclear distribution around the SS region at $T = 500$ K is more broad than that at $T = 300$ K (see Fig. 5). This suggests that the asynchronous process becomes more important as the temperature increases.

It should be mentioned that the mechanism of the double proton transfer process is strongly dependent on the absolute values of the barrier heights of the concerted and stepwise processes. In the case of porphycene, all previous electronic structure calculations using DFT and ab initio MP2 methods show that the barrier height of the concerted pathway is larger than that of the stepwise pathway and that the energy difference is only a few kcal/mol (see Table 2). Thus, after the zero-point vibrational correction, the barrier height of the concerted pathway becomes smaller than that of the stepwise pathway. It is well-known that the energetics for porphycene is somewhat different from the porphyrin case. In the case of porphyrin, a previous study shows that the barrier height for the concerted pathway (~24 kcal/mol) is much larger than that for the stepwise pathway (~16 kcal/mol) [19]. It has been concluded that the favorable pathway is that of a stepwise reaction for the tautomerism of porphyrin. Presumably, the computationally demanding size of the porphycene (or porphyrin) molecule indicates that the energetics conclusion may not be regarded as final. In fact, it is frequently pointed out that DFT methods often give lower proton transfer barriers compared to ab initio molecular orbital theory methods. Accurate estimation of the relative energies of the stationary points of porphycene should be one of the important future directions from the electronic structure

viewpoint. In addition, vibrational energies including anharmonicity would also be estimated at an accurate level for quantitative discussion.

Another important future direction is to extend the present PIMD simulations to an isotopically substituted porphycene. Very recently, Vdovin et al. [20] have found that a singly deuterated porphycene molecule embedded in low-temperature helium droplets shows the tunneling doublets in the measured spectrum although the corresponding splitting value is much smaller than that for protonated porphycene. They have concluded that the tunneling doublets observed are indicative for the concerted mechanism even when one of the inner protons is isopotically substituted. It may be very interesting to study how the double proton transfer mechanism changes upon isotope substitution in PIMD simulations. Such a computational study is currently in progress in our laboratory.

Acknowledgement

References

[1] K. Giese, M. Petković, H. Naundorf, O. Kühn, Phys. Rep. 430 (2006) 211.
[2] J.T. Hynes, J.P. Klinman, H.-H. Limbach, R.L. Schowen (Eds.), Hydrogen-Transfer Reactions, Wiley-VCH, Weinheim, 2007.
[3] Y.-D. Wu, K.W.K. Chan, C.-P. Yip, E. Vogel, D.A. Plattner, K.N. Houk, J. Org. Chem. 62 (1997) 9240.
[4] K. Malsch, G. Hohlneicher, J. Phys. Chem. A 101 (1997) 8409.
[5] M. Boronat, E. Ortí, P.M. Viruela, F. Tomás, J. Mol. Struct. (Theochem.) 390 (1997) 149.
[6] P.M. Kozlowski, M.Z. Zgierski, J. Baker, J. Chem. Phys. 109 (1998) 5905.
[7] M.F. Shibl, M. Tachikawa, O. Kühn, Phys. Chem. Chem. Phys. 7 (2005) 1368.
[8] H. Cybulski, M. Pecul, T. Helgaker, M. Jaszuński, J. Phys. Chem. A 109 (2005) 4162.
[9] T. Udagawa, M. Tachikawa, J. Chem. Phys. 125 (2006) 244105.
[10] Ł. Walewski, D. Krachtus, S. Fischer, J.C. Smith, P. Bała, B. Lesyng, Int. J. Quant. Chem. 106 (2006) 636.
[11] Z. Smedarchina, M.F. Shibl, O. Kühn, A. Fernández-Ramos, Chem. Phys. Lett. 436 (2007) 314.
[12] Ł. Walewski, P. Bała, B. Lesyng, NIC Ser. 36 (2007) 291.
[13] M.F. Shibl, M. Pietrzak, H.-H. Limbach, O. Kühn, ChemPhysChem 8 (2007) 315.
[14] Ł. Walewski, J. Waluk, B. Lesyng, J. Phys. Chem. A 114 (2010) 2313.
[15] B. Wehrle, H.-H. Limbach, M. Köcher, O. Ermer, E. Vogel, Angew. Chem. Int. Ed. Engl. 26 (1987) 934.
[16] J. Waluk, M. Müller, P. Swiderek, M. Köcher, E. Vogel, G. Hohlneicher, J. Michl, J. Am. Chem. Soc. 113 (1991) 5511.
[17] J. Sepioł, Y. Stepanenko, A. Vdovin, A. Mordziński, E. Vogel, J. Waluk, Chem. Phys. Lett. 296 (1998) 549.
[18] A. Vdovin, J. Sepioł, N. Urbańska, M. Pietraszkiewicz, A. Mordziński, J. Waluk, J. Am. Chem. Soc. 128 (2006) 2577.
[19] M. Gil, J. Waluk, J. Am. Chem. Soc. 129 (2007) 1335.
[20] A. Vdovin, J. Waluk, B. Dick, A. Slenczka, ChemPhysChem 10 (2009) 761.
[21] E. Vogel, M. Köcher, H. Schmickler, J. Lex, Angew. Chem. Int. Ed. Engl. 25 (1986) 257.
[22] D. Marx, M. Parrinello, Z. Phys. B 95 (1994) 143.
[23] M. Shiga, M. Tachikawa, S. Miura, Chem. Phys. Lett. 332 (2000) 396.
[24] M. Shiga, M. Tachikawa, S. Miura, J. Chem. Phys. 115 (2001) 9149.
[25] M. Shiga, M. Tachikawa, Chem. Phys. Lett. 374 (2003) 229.
[26] A. Gonzalez-Lafont, T.N. Truong, D.G. Truhlar, J. Phys. Chem. 95 (1991) 4618.
[27] Y.-P. Liu, D.-H. Lu, A. Gonzalez-Lafont, D.G. Truhlar, B.C. Garrett, J. Am. Chem. Soc. 115 (1993) 7806.
[28] I. Rossi, D.G. Truhlar, Chem. Phys. Lett. 233 (1995) 231.
[29] J.J.P. Stewart, J. Mol. Model. 13 (2007) 1173.
[30] K. Malsch, M. Roeb, V. Karuth, G. Hohlneicher, Chem. Phys. 227 (1998) 331.
[31] M.J. Frisch et al., GAUSSIAN-03, Revision D.02, Gaussian Inc., Wallingford, CT, 2004.
[32] B.J. Berne, D. Thirumalai, Ann. Rev. Phys. Chem. 37 (1986) 401.
[33] MOPAC2007, James J.P. Stewart, Stewart Computational Chemistry, Colorado Springs, CO, USA, 2007. <http://OpenMOPAC.net>.
[34] U.W. Schmitt, G.A. Voth, J. Chem. Phys. 111 (1999) 9361.